Cross second virial coefficients and dilute gas transport properties of the (CH_4 + CO_2), (CH_4 + H_2S), and (H_2S + CO_2) systems from accurate intermolecular potential energy surfaces

Robert Hellmann*, Eckard Bich

Institut für Chemie, Universität Rostock, 18059 Rostock, Germany

Velisa Vesovic

Department of Earth Science and Engineering, Imperial College London, London SW7 2AZ, UK

Abstract

The cross second virial coefficient and the dilute gas shear viscosity, thermal conductivity, and binary diffusion coefficient have been calculated for (CH_4 + CO_2), (CH_4 + H_2S), and (H_2S + CO_2) mixtures in the temperature range from (150 to 1200) K. The cross second virial coefficient was obtained using the Mayer-sampling Monte Carlo approach, while the transport properties were evaluated by means of the classical trajectory method. State-of-the-art intermolecular potential energy surfaces for the like and unlike species interactions were employed in the calculations. All potential energy surfaces are based on highly accurate quantum-chemical *ab initio* calculations, with the potentials for the unlike interactions reported in this work and those for the like interactions taken from our previous studies of the pure gases. The computed transport property values are in good agreement with the few available experimental data, which are limited to (CH_4 + CO_2) mixtures close to room temperature. The lack of reliable data makes the values of the thermophysical properties calculated in this work currently the most accurate estimates for low-density (CH_4 + CO_2), (CH_4 + H_2S), and (H_2S + CO_2) mixtures. Tables of recommended values for all investigated thermophysical properties as a function of temperature and composition are provided.

Keywords: potential energy surface, methane, carbon dioxide, hydrogen sulphide, second virial coefficient, transport properties

The Version of Record is available at http://dx.doi.org/10.1016/j.jct.2016.07.034.

*Corresponding author

Email addresses: robert.hellmann@uni-rostock.de (Robert Hellmann), eckard.bich@uni-rostock.de (Eckard Bich), v.vesovic@imperial.ac.uk (Velisa Vesovic)

1. Introduction

There is considerable industrial demand for accurate and reliable values of thermophysical properties of a wide variety of fluids over extensive ranges of temperature and pressure as has been demonstrated in a number of studies [1]. The economic case for improving the accuracy with which the properties are determined is strong; however, the wide range of possible fluids and their mixtures and of conditions of interest precludes obtaining the relevant data by experimental means alone. There is, therefore, a clear need for predictive methods and calculations that produce accurate, reliable, and internally consistent data. In this context, the thermophysical properties in the dilute gas limit (i.e., in the limit of zero density) provide the essential basis for the correlation and prediction of the properties over a wider range of thermodynamic states [2].

The macroscopic properties of a dilute gas are governed by binary molecular interactions, and the recent computational advances in the field have allowed us not only to accurately determine the intermolecular potential energy surfaces (PESs) using quantum-chemical *ab initio* methods [3–6], but also to calculate the transport properties by making use of a rigorous molecular description [7, 8]. Such calculations have been performed for a number of simple gases, such as methane [9, 10], carbon dioxide [5], hydrogen sulfide [4, 11], water vapor [12, 13], and ethylene oxide [6], yielding transport property values with an uncertainty commensurate with the best experimental measurements over wide temperature ranges. We have recently extended the calculations to binary mixtures and have reported values for three traditional transport properties (viscosity, thermal conductivity, binary diffusion coefficient) and for the cross second virial coefficient of (CH_4 + N_2) mixtures [8, 14]. The objective of this paper is to extend the study to include (CH_4 + CO_2), (CH_4 + H_2S), and (H_2S + CO_2) mixtures. By providing values of the aforementioned thermophysical properties for these mixtures, we aim to fill an existing data gap as the available experimental measurements are meager, even at room temperature. The calculated values are intended not only to fully characterize the aforementioned mixtures, but also to serve as benchmark data for testing different prediction methods for low-density gaseous systems.

The choice of mixtures was, to a certain extent, determined by the previous work on pure gases and by current limitations of theory and lack of computing power to extend the calculations to larger molecules. Nevertheless, the mixtures chosen form a vital subset of industrially relevant fluids. Methane, nitrogen, carbon dioxide, and hydrogen sulfide are important constituents of natural gas, which is seen as a transitional energy source in moving towards cleaner energy and is also a critical raw material in gas-to-liquids processes. Its usage is expected not only to grow, but diversify [15]. The increasing preponderance of sour natural gas and natural gas with a high CO_2 content from pre-salt fields in the supply market will require the development of further treatments for the removal of H_2S and CO_2 [16]. The provision of accurate and reliable thermophysical property data forms an important element not only in optimizing natural gas utilization, but also in Carbon Capture and Storage (CCS), which relies on treating and injecting CO_2 streams that are never pure but contain CH_4, H_2S, and N_2 among the impurities. Gas processing using membranes [17], where diffusion coefficients and viscosity play an important part, also involves mixtures that contain the four components for which we have calculated the thermophysical properties.

The cross second virial coefficients are determined solely by the respective PESs for the unlike interactions. Two *ab initio* potentials are available in the literature for the CH_4–CO_2 molecule pair [18, 19]. Oakley et al. [18] calculated the interaction energies only at the MP2 level of theory, which is not accurate enough for the present purpose. Pai and Bae [19] used the much more accurate CCSD(T) method [20]. However, for efficiency they fitted a relatively simple analytical function to their computed interaction energies, resulting in large fitting errors. We could have improved their PES by fitting a more accurate analytical function, but when the paper of Pai and Bae was published, we had already completed the development of our own PES, which is presented in this paper. For the CH_4–H_2S interaction, the only available PES based on *ab initio* calculated interaction energies is that of Woon et al. [21], which was published in 1990. It is based on a fit to only 38 interaction energies, which were computed at the MP2 level with very small basis sets by today's standards. For the H_2S–CO_2 molecule pair, no *ab initio* PES has been developed so far. We therefore also present new PESs for the latter two molecule pairs in the present paper.

To calculate the transport properties of the mixtures in the dilute gas limit, PESs for the CH_4–CH_4, CO_2–CO_2, and H_2S–H_2S interactions are also required. We have previously developed such potentials [3–5] to investigate the thermophysical properties of these three pure gases [3–5, 9–11].

The cross second virial coefficients have been calculated using the Mayer-sampling Monte Carlo (MSMC) approach [22]. To account for quantum effects semiclassically, the quadratic Feynman–Hibbs (QFH) effective pair potential [23] was utilized. Transport properties in the dilute gas limit have been determined by means of the classical trajectory approach in conjunction with the kinetic theory of molecular gases [8, 14, 24–26]. The accuracy and usefulness of this approach has been demonstrated for several pure molecular gases and gas mixtures, see, for example, Refs. [5–8, 12–14]. The calculation of all thermophysical properties presented in this work was performed in the temperature range from (150 to 1200) K.

In Section 2, the *ab initio* calculations for the CH_4–CO_2, CH_4–H_2S, and H_2S–CO_2 molecule pairs and the analytical potential functions are described. In Section 3, the methodology for the calculation of the cross second virial coefficients and transport properties is presented, while in Section 4 the results are discussed and compared with experimental data. A summary and conclusions are given in Section 5.

2. Intermolecular potential energy surfaces for the CH_4–CO_2, CH_4–H_2S, and H_2S–CO_2 molecule pairs

2.1. Ab initio calculations

The CH_4, CO_2, and H_2S molecules were treated as rigid rotors in all *ab initio* calculations. In accordance with our intermolecular PESs for the pure components [3–5], we used CH, CO, and SH bond lengths of 109.90 pm, 116.25 pm, and 135.06 pm, respectively, and HCH, OCO, and HSH bond angles of 109.471°, 180°, and 92.219°, respectively. These values correspond to the zero-point vibrationally averaged geometries. Within the rigid-rotor approximation, each configuration of two molecules can be defined by the distance between the centers of mass of the molecules, R,

as well as four angles for the CH_4–CO_2 and H_2S–CO_2 molecule pairs and five angles for the CH_4–H_2S molecule pair. Details concerning the precise definition of these angles can be found in the Supplementary information.

For the development of the CH_4–CO_2 potential, 43 distinct angular orientations of the two molecules were considered. The number of center-of-mass separations R for each angular orientation varied from 12 in the range 0.35 nm $\leqslant R \leqslant$ 1.0 nm to 19 in the range 0.175 nm $\leqslant R \leqslant$ 1.0 nm. This resulted in a total of 707 CH_4–CO_2 configurations. For the CH_4–H_2S potential, 167 angular orientations with up to ten center-of-mass separations in the range 0.25 nm $\leqslant R \leqslant$ 0.9 nm were considered, resulting in 1645 configurations. For the development of the H_2S–CO_2 potential, 233 angular orientations with up to 16 center-of-mass separations in the range 0.2 nm $\leqslant R \leqslant$ 1.0 nm, in total 3546 configurations, were considered. The increase in the number of angular orientations is necessary due to H_2S having a lower symmetry compared with both the CH_4 and CO_2 molecules.

The interaction energies, V, for all three molecule pairs were computed utilizing the supermolecular approach including the full counterpoise correction [27] at the frozen-core CCSD(T) [20] level of theory using the aug-cc-pVXZ (aug-cc-pV($X+d$)Z for sulfur) basis sets with $X = 3$ (T) and $X = 4$ (Q) [28–30]. The basis sets were supplemented by a small $3s3p2d1f$ set of bond functions located midway along the R axis with exponents of 0.1, 0.3, and 0.9 for s and p, 0.25 and 0.75 for d, and 0.45 for f. The correlation contributions to the interaction energies, $V_{\mathrm{CCSD(T)\,corr}}$, were extrapolated to the complete basis set (CBS) limit using the two-point scheme recommended by Halkier et al. [31],

$$V_{\mathrm{CCSD(T)\,corr}}(X) = V^{\mathrm{CBS}}_{\mathrm{CCSD(T)\,corr}} + \alpha\, X^{-3}. \tag{1}$$

Because the Hartree–Fock self-consistent-field (SCF) contributions converge much faster to the CBS limit than the correlation contributions, we used the SCF interaction energies resulting from the CCSD(T) computations with $X = 4$ to approximate the CBS limit.

The results of the quantum-chemical *ab initio* calculations for all configurations of the CH_4–CO_2, CH_4–H_2S, and H_2S–CO_2 molecule pairs can be found in the Supplementary material. All *ab initio* calculations were performed using the CFOUR program [32].

2.2. *Analytical potential functions*

In accordance with our previous work on the CH_4–CH_4, CO_2–CO_2, and H_2S–H_2S PESs [3–5], we fitted site-site potential functions with nine sites for CH_4, seven sites for CO_2, and 11 sites for H_2S to the calculated interaction energies at the CCSD(T)/CBS level. Each individual site-site interaction is represented by a simple function that depends only on the distance R_{ij} between site i in molecule 1 and site j in molecule 2,

$$V_{ij}(R_{ij}) = A_{ij}\exp(-\alpha_{ij}R_{ij}) - f_6(b_{ij},R_{ij})\frac{C_{6\,ij}}{R_{ij}^6} + \frac{q_i q_j}{R_{ij}}, \tag{2}$$

where f_6 is a damping function [33],

$$f_6(b_{ij},R_{ij}) = 1 - \exp(-b_{ij}R_{ij})\sum_{k=0}^{6}\frac{(b_{ij}R_{ij})^k}{k!}. \tag{3}$$

The total interaction energy is obtained as the sum over all site-site interactions between molecules 1 and 2,

$$V = \sum_i \sum_j V_{ij}(R_{ij}). \tag{4}$$

The positions and partial charges q of the sites were taken from our previous work [3–5]. The number of symmetry-distinct sites per molecule is three for CH_4, four for CO_2, and seven for H_2S. This results in 12, 21, and 28 types of site-site interactions for the CH_4–CO_2, CH_4–H_2S, and H_2S–CO_2 molecule pairs, respectively. The parameters A, α, b, and C_6 for the different types of interactions were fully optimized in non-linear least-squares fits. Thus, a total of 48, 84, and 112 parameters were optimized for the CH_4–CO_2, CH_4–H_2S, and H_2S–CO_2 molecule pairs, respectively.

Figure 1 shows the deviations of the fitted interaction energies for all three PESs from the corresponding *ab initio* calculated values as a function of the latter up to 8000 K. As can be seen in the figure, most of the deviations are within ±2%, which is excellent in the context of fitting multi-dimensional analytical functions to *ab initio* calculated interaction energies. The three PESs are strongly anisotropic. As an illustrative example, the distance dependence of the *ab initio* calculated CH_4–CO_2 interaction energies and of the fitted analytical potential function is shown for selected angular orientations in figure 2. The analytical PES exhibits only one distinct equilibrium structure with $V = -500.0$ K. It corresponds very closely to the minimum of the lowest curve in figure 2. The CH_4–H_2S PES features two distinct equilibrium structures with $V = -397.1$ K and $V = -455.7$ K, and the H_2S–CO_2 PES exhibits one distinct equilibrium structure with $V = -861.5$ K.

In our studies of the CH_4–CH_4 [3] and CH_4–N_2 [14] potentials, we also used zero-point vibrationally averaged monomer geometries and applied the highly accurate CCSD(T) method in combination with extrapolation to the CBS limit for the calculation of the interaction energies. However, despite the high level of theory, the calculated values for both the second virial coefficient of pure CH_4 and the CH_4–N_2 cross second virial coefficient turned out to be systematically too positive in comparison with most of the experimental data. The main reason for this is that using vibrationally averaged monomer geometries only partly accounts for vibrational effects on the interaction energies. Particularly for the CH_4 molecule, vibrations strongly increase the polarizability [34, 35] and hence the strength of dispersion interactions involving CH_4 [36]. However, by adjusting only one dispersion-related parameter for each PES, we were able to achieve excellent agreement with the best experimental data over wide temperature ranges [3, 14]. For the CH_4–CO_2 and CH_4–H_2S potentials, we have performed a similar fine tuning by adjusting the C_6 fitting parameter for the site-site interaction between the carbon atoms of CH_4 and CO_2 and for the site-site interaction between the carbon atom of CH_4 and the site closest to the center of mass of H_2S. The adjustment procedure, which is discussed further in Sections 4.1.1 and 4.1.2, changes the interaction energies for the equilibrium structures to $V = -509.1$ K for the CH_4–CO_2 PES and to $V = -402.6$ K and $V = -464.2$ K for the CH_4–H_2S PES. No adjustments were made for the H_2S–CO_2 potential.

The parameters of the analytical potential functions, the interaction energies calculated with these functions for all investigated configurations of the three molecule pairs, Fortran 90 routines of the potential functions, as well as details of the equilibrium geometries are provided in the Supplementary material.

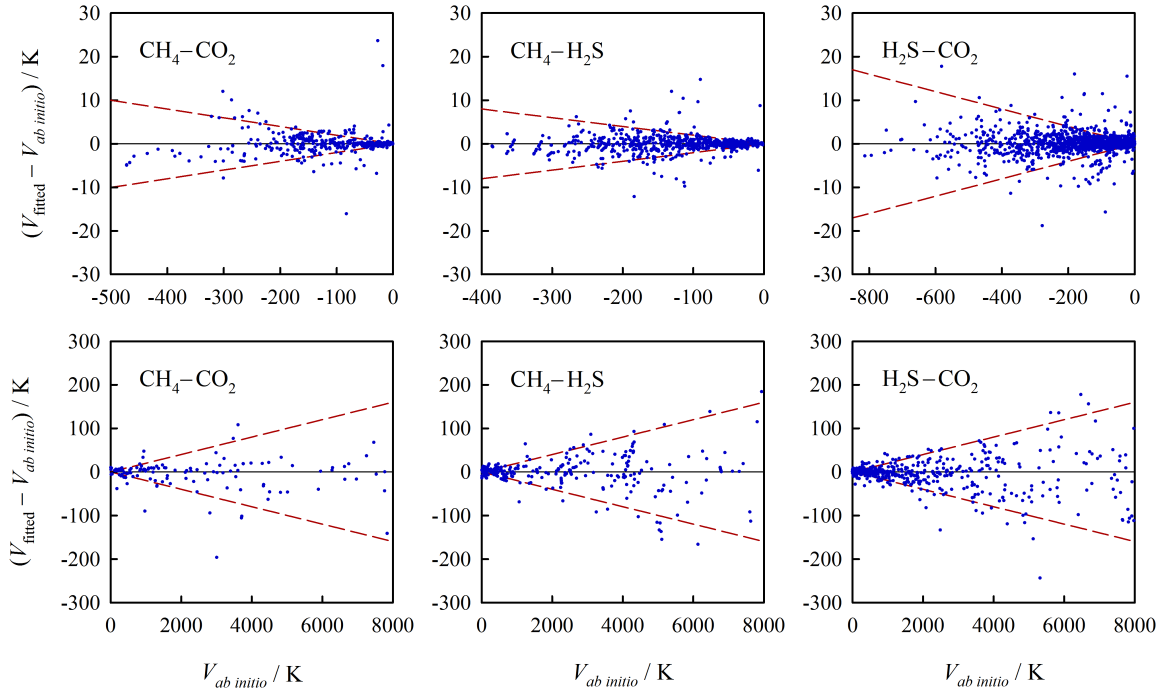

Figure 1: Deviations of interaction energies obtained using the fitted analytical CH_4–CO_2, CH_4–H_2S, and H_2S–CO_2 potential functions from the corresponding *ab initio* calculated values as a function of the latter. The dashed lines indicate relative deviations of ±2%.

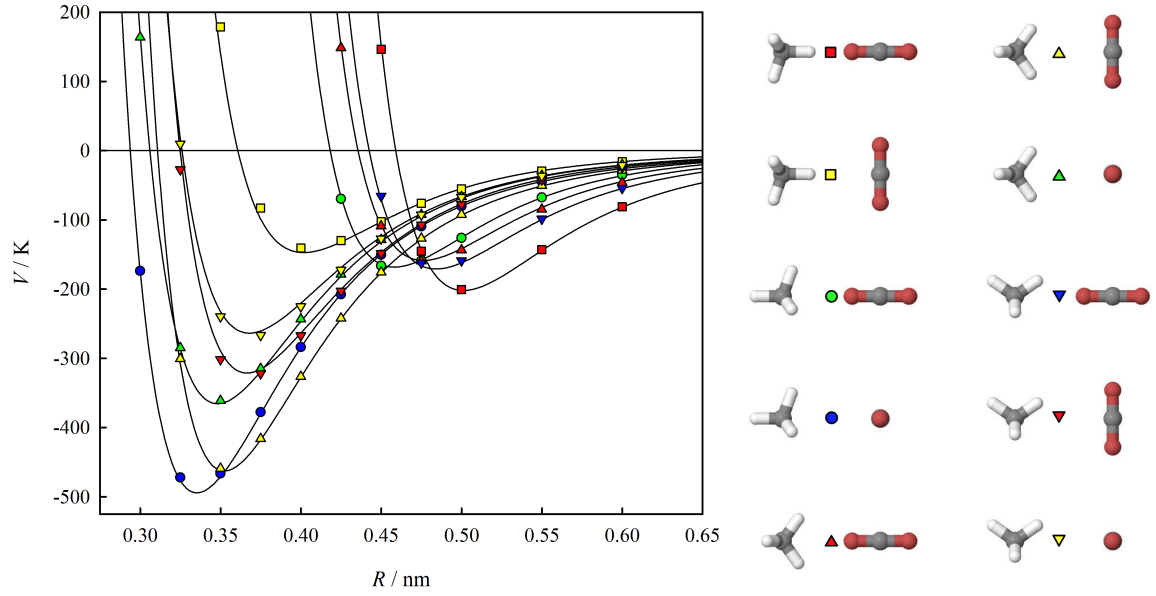

Figure 2: CH_4–CO_2 pair potential as a function of the center-of-mass distance R for ten of the 43 considered angular orientations. The *ab initio* calculated values are represented by symbols and the fitted analytical potential function by solid lines.

3. Calculation of thermophysical properties

3.1. Cross second virial coefficients

The classical cross second virial coefficient for rigid molecules as a function of temperature is given as

$$B_{12}^{\mathrm{cl}} = -\frac{N_{\mathrm{A}}}{2}\int_0^\infty \langle f_{12}\rangle_{\Omega_1,\Omega_2}\mathrm{d}\mathbf{R}, \tag{5}$$

with

$$f_{12} = \exp\left[-\frac{V(\mathbf{R},\Omega_1,\Omega_2)}{k_{\mathrm{B}}T}\right] - 1, \tag{6}$$

where N_{A} is Avogadro's constant, k_{B} is Boltzmann's constant, $\mathbf{R}$ is the distance vector between the centers of mass of the two molecules, Ω_1 and Ω_2 represent the angular orientations of molecules 1 and 2, respectively, and the angle brackets denote averages over Ω_1 and Ω_2. Quantum effects can be taken into account semiclassically by replacing the pair potential V in Equation (6) by the QFH effective pair potential [23]. For a molecule pair consisting of a spherical top and a linear molecule, such as the CH_4–CO_2 molecule pair, the QFH potential can be written as follows [14]:

$$V_{\mathrm{QFH}} = V + \frac{\hbar^2}{24k_{\mathrm{B}}T}\left[\frac{1}{\mu}\left(\frac{\partial^2 V}{\partial x^2}+\frac{\partial^2 V}{\partial y^2}+\frac{\partial^2 V}{\partial z^2}\right)+\frac{1}{I_1}\left(\frac{\partial^2 V}{\partial \psi_{1,a}^2}+\frac{\partial^2 V}{\partial \psi_{1,b}^2}+\frac{\partial^2 V}{\partial \psi_{1,c}^2}\right)+\frac{1}{I_2}\left(\frac{\partial^2 V}{\partial \psi_{2,a}^2}+\frac{\partial^2 V}{\partial \psi_{2,b}^2}\right)\right], \tag{7}$$

where $\hbar$ is Planck's constant divided by 2π, μ is the reduced mass of the molecule pair, x, y, z are the Cartesian components of $\mathbf{R}$, I_1 and I_2 are the moments of inertia of molecules 1 (CH_4) and 2 (CO_2), the angles $\psi_{1,a}$, $\psi_{1,b}$, $\psi_{1,c}$ correspond to rotations around the principal axes of CH_4, and $\psi_{2,a}$ and $\psi_{2,b}$ are the corresponding angles for CO_2. The expressions for the CH_4–H_2S and H_2S–CO_2 molecule pairs are similar in structure; the expression for the rotational contribution of an asymmetric top (H_2S) can be found, for example, in Ref. [6].

To calculate the cross second virial coefficients, we applied the MSMC approach of Singh and Kofke [22], which we also used in several of our previous studies. For all three molecule pairs, the cross second virial coefficient was computed at 46 temperatures from (150 to 1200) K as well as at all temperatures for which experimental data are available. The hard-sphere fluid with a sphere diameter of 0.45 nm was used as reference system. Results for all temperatures were obtained simultaneously by performing multi-temperature simulations [22, 37] with a sampling temperature of 150 K and 2×10^{10} trial moves. For each trial move, one of the molecules was displaced and rotated. Maximum step sizes for the moves were adjusted in short equilibration periods to achieve acceptance rates of 50%. The second derivatives required for evaluating the QFH potentials were evaluated analytically. For each molecule pair, the computed virial coefficients from eight independent simulation runs were averaged. The standard uncertainty of the computed values due to the Monte Carlo integration is smaller than 0.05 $\mathrm{cm^3 \cdot mol^{-1}}$ for all molecule pairs and temperatures.

3.2. Transport properties

The transport properties of dilute gas mixtures can be calculated using the kinetic theory of polyatomic gases [8, 14, 24–26, 38–42]. For each transport coefficient, a system of linear equations needs to be solved. The approaches

employed in the present work for the calculation of the shear viscosity η, the thermal conductivity λ (under steady-state conditions, see Ref. [8] for details), and the product of the molar density and the binary diffusion coefficient, $\rho_m D$, are the same as in our studies of the (CH_4 + N_2) system [8, 14]. For completeness, we present the approach for viscosity here and refer the reader to Refs. [14] and [8] for the details concerning the other two transport properties. We note that there is an error in the final expression for the mixture viscosity in Ref. [14]. The right hand side of Equation (12) therein has to be multiplied by the factor C^{2000}. However, the calculations were performed using the correct expression.

For the shear viscosity η of a dilute binary gas mixture consisting of species A and B, the system of linear equations is given as

$$\begin{aligned}
\sum_{p'q's't'} \left[\bar{S}\begin{pmatrix} p & q & s & t \\ p' & q' & s' & t' \end{pmatrix}^{(2)}_{\mathrm{AA}} X_{\mathrm{A}}^{p'q's't'} + \bar{S}\begin{pmatrix} p & q & s & t \\ p' & q' & s' & t' \end{pmatrix}^{(2)}_{\mathrm{AB}} X_{\mathrm{B}}^{p'q's't'} \right] &= \delta_{p2}\delta_{q0}\delta_{s0}\delta_{t0}\, x_{\mathrm{A}} C^{2000}, \\
\sum_{p'q's't'} \left[\bar{S}\begin{pmatrix} p & q & s & t \\ p' & q' & s' & t' \end{pmatrix}^{(2)}_{\mathrm{BA}} X_{\mathrm{A}}^{p'q's't'} + \bar{S}\begin{pmatrix} p & q & s & t \\ p' & q' & s' & t' \end{pmatrix}^{(2)}_{\mathrm{BB}} X_{\mathrm{B}}^{p'q's't'} \right] &= \delta_{p2}\delta_{q0}\delta_{s0}\delta_{t0}\, x_{\mathrm{B}} C^{2000},
\end{aligned} \tag{8}$$

where δ_{ij} is the Kronecker delta, x_{A} and x_{B} are the mole fractions, $X_{\mathrm{A}}^{p'q's't'}$ and $X_{\mathrm{B}}^{p'q's't'}$ are the resulting solutions of the coupled set of equations, and $C^{2000} = \sqrt{2}$. The coefficients $\bar{S}\left(\begin{smallmatrix} p & q & s & t \\ p' & q' & s' & t' \end{smallmatrix}\right)^{(k)}_{\alpha\beta}$ are given by

$$\bar{S}\begin{pmatrix} p & q & s & t \\ p' & q' & s' & t' \end{pmatrix}^{(k)}_{\alpha\beta} = \delta_{\alpha\beta} \sum_{\gamma} x_\alpha x_\gamma \langle v \rangle_{\alpha\gamma} \bar{\sigma}'\begin{pmatrix} p & q & s & t \\ p' & q' & s' & t' \end{pmatrix}^{(k)}_{\alpha\gamma} + x_\alpha x_\beta \langle v \rangle_{\alpha\beta} \bar{\sigma}''\begin{pmatrix} p & q & s & t \\ p' & q' & s' & t' \end{pmatrix}^{(k)}_{\alpha\beta}, \tag{9}$$

where $\langle v \rangle_{\alpha\beta} = (8 k_{\mathrm{B}} T / \pi \mu_{\alpha\beta})^{1/2}$ is the average relative thermal speed of molecules of types α and β, $\mu_{\alpha\beta}$ is their reduced mass, and the index γ runs over both mixture components. The quantities $\bar{\sigma}'\left(\begin{smallmatrix} p & q & s & t \\ p' & q' & s' & t' \end{smallmatrix}\right)^{(k)}_{\alpha\beta}$ and $\bar{\sigma}''\left(\begin{smallmatrix} p & q & s & t \\ p' & q' & s' & t' \end{smallmatrix}\right)^{(k)}_{\alpha\beta}$ are temperature-dependent generalized cross sections in the laboratory frame [14, 24, 26, 41]. They are determined by the binary collisions in the gas mixture and are therefore directly related to the intermolecular pair potentials. Apart from the overbar and the added species subscripts, the present notation for the generalized cross sections is identical to that of Curtiss [41]. The shear viscosity is obtained as

$$\eta = \frac{1}{2} k_{\mathrm{B}} T C^{2000} \left(x_{\mathrm{A}} X_{\mathrm{A}}^{2000} + x_{\mathrm{B}} X_{\mathrm{B}}^{2000} \right). \tag{10}$$

To calculate the first-order approximation for η, only a single set of $pqst$ and $p'q's't'$ values needs to be considered in the system of linear equations (8), $(pqst) = (p'q's't') = (2000)$. The second-order approximation traditionally includes the sets (2000), (2010), (2001), and (0200) [43]. In this work, we used a third-order approximation [5, 14] that adds the sets (2020), (2011), (2002), (2100), and (2200) to those for the second-order approximation, resulting in 18 coupled equations.

The thermal conductivity and the binary diffusion coefficient were calculated using second- and third-order approximations, respectively [8, 14]. We note that our approach for the calculation of the thermal conductivity [8] fully accounts for the coupling between the translational and rotational degrees of freedom, whereas the vibrational states of the molecules are assumed to be "frozen," i.e., unaffected by collisions. The approach requires knowledge of the

vibrational contributions to the ideal gas heat capacities of the pure gases. They were obtained from the most accurate equations of state available for the three fluids [44–46].

The generalized cross sections for the CH_4–CO_2, CH_4–H_2S, and H_2S–CO_2 binary collisions were computed within the rigid-rotor approximation by means of the classical trajectory method using an extended version of the TRAJECT software code [14, 25, 26]. The trajectories were obtained by integrating Hamilton's equations from pre- to post-collisional values with an initial and final separation of 50 nm. Total-energy-dependent generalized cross sections in the center-of-mass frame, which are integrals over the initial states of the trajectories, were calculated for 27 values of the total energy, $E_{tot} = E_{tr} + E_{rot}$, in the range from (50 to 25 000) K by means of a simple Monte Carlo scheme utilizing quasi-random numbers. For each molecule pair, up to 4×10^6 trajectories were computed at each total energy value. For $E_{tot} < 250$ K, the number of trajectories had to be reduced because the computational demand required to calculate a trajectory with sufficient accuracy increases with decreasing energy. For example, only 100 000 trajectories were calculated at $E_{tot} = 50$ K. However, the contributions of such low energies to the transport properties at temperatures above 150 K are negligibly small. An integration over the total energy, which was performed using Chebyshev quadrature, yielded temperature-dependent generalized cross sections in the center-of-mass frame [26]. Finally, the center-of-mass cross sections were converted to laboratory frame cross sections [26, 41].

Generalized cross sections for CH_4–CH_4, CO_2–CO_2, and H_2S–H_2S collisions, which are also required for the calculation of the transport properties of the mixtures, were obtained from the potentials of Refs. [3–5] using a similar procedure. The details of these calculations have been described in earlier papers [4, 5, 12, 14] and are therefore not repeated here. In the present work, we used the set of H_2S–H_2S cross sections of Ref. [12] instead of the older, slightly less accurate set of Ref. [4].

The relative standard uncertainty of the computed values for viscosity, thermal conductivity, and binary diffusion coefficient due to the Monte Carlo integration scheme employed in the classical trajectory method is estimated (based on the uncertainty estimates generated by TRAJECT for the individual cross sections [25]) to be smaller than 0.2% at all temperatures and compositions of the investigated systems. The uncertainties due to the numerical integration of Hamilton's equations and due to the integration over the total energy using Chebyshev quadrature are negligible.

4. Results and discussion

4.1. Cross second virial coefficients

The calculated semiclassical values for the cross second virial coefficients of the three molecule pairs and our estimates of their combined expanded (coverage factor $k = 2$ or approximately 95% confidence level) uncertainties (discussed below) are given in Table 1. The listed CH_4–CO_2 and CH_4–H_2S values are those for the adjusted potentials.

4.1.1. CH_4–CO_2 molecule pair

In figure 3, the calculated values for the cross second virial coefficient of the CH_4–CO_2 molecule pair are compared with selected experimental data [47–56] and with the correlation of Dymond et al. [57]. The data of Ng [48] were

taken from Ref. [57]. We reanalyzed the data of Martin et al. [51] and of Esper et al. [53] using more accurate values of the pure-component virial coefficients [3, 5]. This resulted in changes of at most +0.60 $cm^3 \cdot mol^{-1}$ for the former and −0.36 $cm^3 \cdot mol^{-1}$ for the latter. The error bars shown in the figure correspond to those given by the authors except for the reanalyzed data of Martin et al., for which we also reanalyzed the uncertainty. We used the reanalyzed data of Martin et al. [51] as well as the data of Jaeschke et al. [52] and of Iglesias-Silva et al. [56] as reference for the adjustment of the analytical potential function (see Section 2.2). To help visualize the deviations, these three data sets are shown as filled symbols in the figure. The semiclassical values of the cross second virial coefficient obtained using the adjusted PES reproduce the three data sets within ±0.5 $cm^3 \cdot mol^{-1}$. The semiclassical values for the unadjusted PES deviate from the corresponding values for the adjusted PES by +9.7 $cm^3 \cdot mol^{-1}$ at 150 K, +2.8 $cm^3 \cdot mol^{-1}$ at 300 K, and +0.6 $cm^3 \cdot mol^{-1}$ at 1200 K. The figure shows that while all experimental data agree within ±5 $cm^3 \cdot mol^{-1}$ with the values resulting from the adjusted potential function, the experimentally based correlation of Dymond et al. [57] for temperatures from (220 to 400) K exhibits large negative deviations at low temperatures, reaching −14.5 $cm^3 \cdot mol^{-1}$ at 220 K. Nevertheless, the correlation is consistent with the calculated values within the expanded ($k = 2$) uncertainty estimates of Dymond et al. [57].

Based on the comparison with the experimental data, we estimate the combined expanded ($k = 2$) uncertainties of the semiclassical values obtained with the adjusted CH_4–CO_2 potential function to be one half the absolute value of the difference between the values obtained with the unadjusted and the adjusted PES or 1.5 $cm^3 \cdot mol^{-1}$, whichever is larger. As can be seen in figure 3, the majority of the experimental data are consistent with this uncertainty estimate.

For completeness, we note that figure 3 also depicts the classical values obtained with the adjusted potential function. They differ from the semiclassical values by −7.7 $cm^3 \cdot mol^{-1}$ at 150 K, −0.9 $cm^3 \cdot mol^{-1}$ at 300 K, and −0.06 $cm^3 \cdot mol^{-1}$ at 1200 K.

4.1.2. CH_4–H_2S molecule pair

The only experimental information available for the (CH_4 + H_2S) system are the data of Bailey et al. [58]. They measured the second virial coefficient of a nearly equimolar mixture ($x_{CH_4} = 0.5073$) at five temperatures in the range from (300 to 500) K. Bailey et al. did not provide uncertainty estimates for their data and did not attempt to extract values for the cross second virial coefficient. Their data for the second virial coefficient of pure hydrogen sulfide given in the same report [58] differ substantially, by −(8.0 to 18.3) $cm^3 \cdot mol^{-1}$, from our calculated values [4, 11]. As such large deviations cannot be explained by the uncertainties of the computed values (which are estimated to be 5 $cm^3 \cdot mol^{-1}$ at 300 K, decreasing to 1 $cm^3 \cdot mol^{-1}$ at 500 K [4, 11]), we are reluctant to utilize the data of Bailey et al. for a fine tuning of the analytical CH_4–H_2S PES. Instead, we base the adjustment on our analysis for the CH_4–CO_2 molecule pair, since the cross second virial coefficients of the CH_4–CO_2 and CH_4–H_2S molecule pairs are of similar magnitude (which is mainly due to the similar well depths of the PESs, see Section 2.2). Therefore, we assume that an optimal adjustment of the CH_4–H_2S PES leads to a similar change in the values for the cross second virial coefficient as for the CH_4–CO_2 PES. In the latter case, the adjustment lowers the cross second virial coefficient by 2.8 $cm^3 \cdot mol^{-1}$

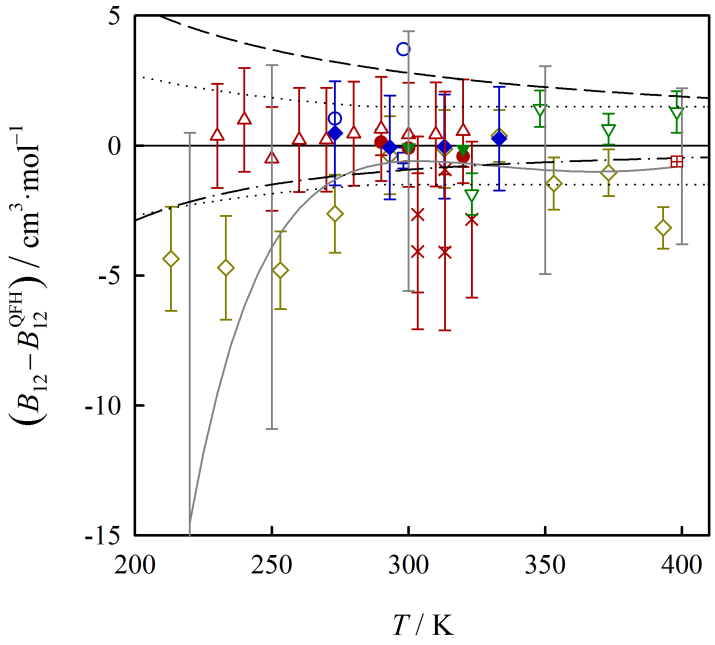

Figure 3: Deviations of experimental data, an experimentally based correlation, and calculated values for the cross second virial coefficient of the CH_4–CO_2 molecule pair from values calculated semiclassically using the adjusted CH_4–CO_2 potential function, B_{12}^{QFH}, as a function of temperature: ○, Brewer [47]; ◇, Ng [48]; □, Katayama et al. [49]; ⊞, Ohgaki et al. [50]; ●, Martin et al. [51], reanalyzed; ◆, Jaeschke et al. [52]; △, Esper et al. [53], reanalyzed; ×, McElroy et al. [54]; ▽, Mallu and Viswanath [55]; ▼, Iglesias-Silva et al. [56]; ——, correlation of Dymond et al. [57]; – – –, semiclassical result for unadjusted CH_4–CO_2 potential function; – · –, classical result for adjusted CH_4–CO_2 potential function; · · · · · ·, $\pm U_{\mathrm{c}}\left(B_{12}^{\mathrm{QFH}}\right)$ with $k = 2$.

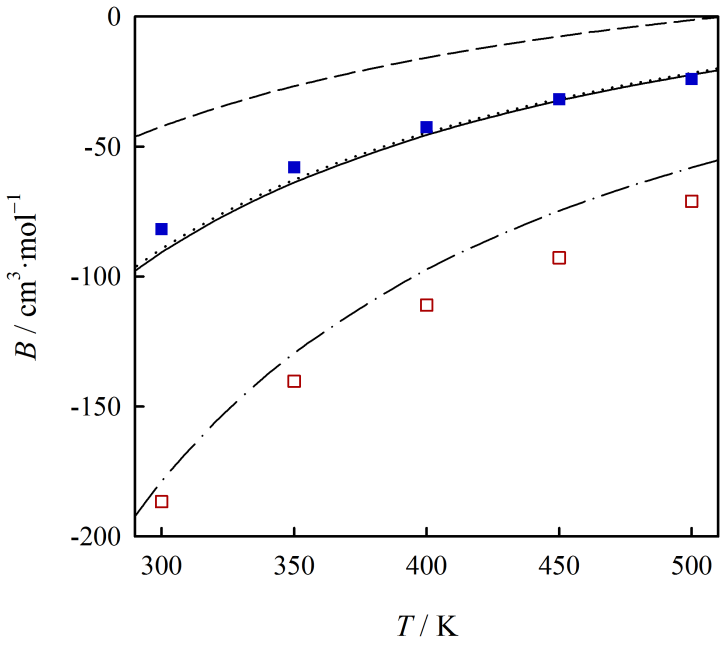

Figure 4: Experimental data and calculated values for the second virial coefficient of a (CH_4 + H_2S) mixture with x_{CH_4} = 0.5073: ■, Bailey et al. [58]; ·····, semiclassical result obtained using the unadjusted CH_4–H_2S potential function; ——, semiclassical result obtained using the adjusted CH_4–H_2S potential function. Calculated values for the second virial coefficient of pure methane: – – –, semiclassical result of Ref. [3]. Experimental data and calculated values for the second virial coefficient of pure hydrogen sulfide: □, Bailey et al. [58]; – · –, semiclassical result of Refs. [4] and [11].

at 300 K, and we adjusted the CH_4–H_2S PES to produce the same effect at this temperature. Figure 4 shows the data of Bailey et al. for a nearly equimolar mixture and for pure hydrogen sulfide as well as the calculated values. The data of Bailey et al. for the mixture deviate by (+7.5 to −2.4) $cm^3 \cdot mol^{-1}$ from the calculated values for the unadjusted PES and by (+8.9 to −1.6) $cm^3 \cdot mol^{-1}$ from those for the adjusted PES.

Taking into account the increased uncertainty due to the rather unsatisfactory fine tuning procedure for the CH_4–H_2S PES, we conservatively estimate the combined expanded (k = 2) uncertainty of the semiclassical values for the cross second virial coefficient obtained with the adjusted potential function to be 1.5 times the absolute value of the difference between the values for the unadjusted and the adjusted PES or 1.5 $cm^3 \cdot mol^{-1}$, whichever is larger.

4.1.3. H_2S–CO_2 molecule pair

In figure 5, the calculated values for the cross second virial coefficient of the H_2S–CO_2 molecule pair are compared with the experimental data of Stouffer et al. [59], who extracted their values from the analysis of the second virial coefficients of several (H_2S + CO_2) mixtures including pure CO_2. The agreement with our semiclassical values is

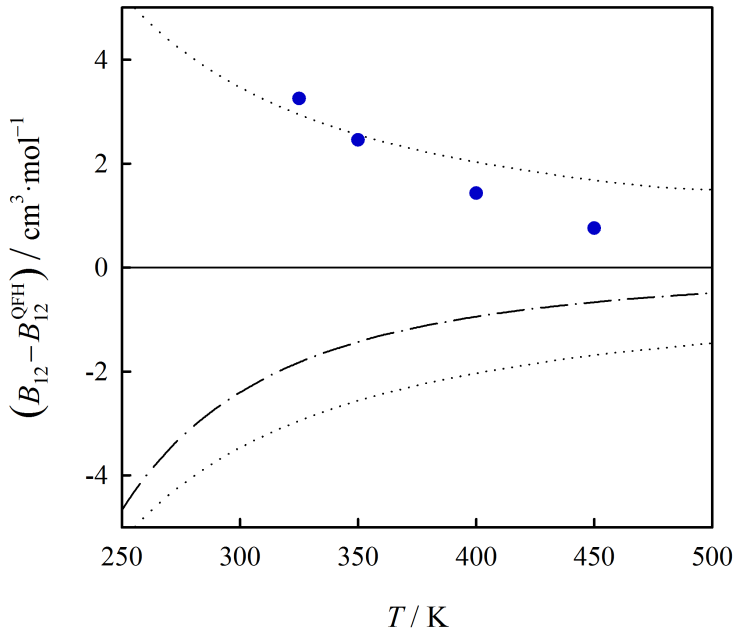

Figure 5: Deviations of experimental data and calculated values for the cross second virial coefficient of the H_2S–CO_2 molecule pair from values calculated semiclassically using the H_2S–CO_2 potential function, B_{12}^{QFH}, as a function of temperature: ●, Stouffer et al. [59]; – · –, classical result; · · · · · ·, $\pm U_c\left(B_{12}^{\mathrm{QFH}}\right)$ with $k = 2$.

satisfactory, with deviations of at most +3.2 cm^3·mol^{-1}. Stouffer et al. did not provide uncertainty estimates for their values.

As we have not adjusted the H_2S–CO_2 PES, we take a different approach to obtain an estimate for the combined expanded ($k = 2$) uncertainty of our calculated values for the H_2S–CO_2 cross second virial coefficient. To estimate the uncertainties due to the basis sets, we fitted the analytical potential function to the calculated H_2S–CO_2 interaction energies at the highest basis set level ($X = 4$, see Section 2.1) without extrapolation to the CBS limit. Taking into account that uncertainties also arise due to the rigid-rotor approximation and the use of the CCSD(T) method in the frozen-core approximation as well as due to the neglect of relativistic effects, we multiply the difference between the cross second virial coefficient values obtained with the two PESs by a factor of two. As for the other two molecule pairs, we set a lower bound of 1.5 cm^3·mol^{-1}.

4.1.4. Correlation

We fitted the coefficients of the following analytical function to the computed semiclassical values for the cross second virial coefficients of the three molecule pairs:

$$\frac{B_{12}^{\mathrm{QFH}}}{\mathrm{cm^3 \cdot mol^{-1}}} = b_0 + \frac{b_{0.5}}{\sqrt{T^*}} + \sum_{i=1}^{6} \frac{b_i}{(T^*)^i}, \tag{11}$$

where $T^* = T/(100\ \mathrm{K})$. The coefficients b are given in Table 2. Equation (11) reproduces the values given in Table 1 to within ±0.003 $\mathrm{cm^3 \cdot mol^{-1}}$, ±0.008 $\mathrm{cm^3 \cdot mol^{-1}}$, and ±0.036 $\mathrm{cm^3 \cdot mol^{-1}}$ for the CH_4–CO_2, CH_4–H_2S, and H_2S–CO_2 molecule pairs, respectively.

4.2. Transport properties

In Table 3, we list the calculated viscosity and thermal conductivity values for the three pure gases at 25 temperatures in the range from (150 to 1200) K. Note that the values for methane and carbon dioxide and most of the thermal conductivity values for hydrogen sulfide listed in the table have been given previously [5, 8, 12, 14]. Calculated values for the viscosities, thermal conductivities, and binary diffusion coefficients of (CH_4 + CO_2), (CH_4 + H_2S), and (H_2S + CO_2) mixtures (using the adjusted versions of the CH_4–CO_2 and CH_4–H_2S PESs) are given in Tables 4–6.

4.2.1. Higher-order kinetic theory approximations

The calculated values for the shear viscosities of pure CH_4, CO_2, and H_2S in the third-order approximation differ from those in the first-order approximation by at most +0.6%, +1.1%, and +0.4%, respectively. As expected, the differences for the binary mixtures lie in between those for the respective pure components. The difference between the third- and second-order results is always smaller than +0.04%. The computed thermal conductivity values in the second-order approximation differ by at most +0.7%, +2.2%, and +0.7% for pure CH_4, CO_2, and H_2S, respectively. The differences for the mixtures lie in between those for the pure components, except for the (CH_4 + H_2S) system, where the differences show only a small variation with composition for a given temperature. We did not calculate the thermal conductivity in the third-order approximation, but we expect the relative differences between third- and second-order results to be similar to those for viscosity. The computed values for the binary diffusion coefficient in the third-order approximation deviate from those in the first-order approximation by no more than +1.2%, +0.9%, and +0.6% for the (CH_4 + CO_2), (CH_4 + H_2S), and (H_2S + CO_2) mixtures, respectively. The third-order contribution does not exceed +0.1%.

4.2.2. Influence of the PES for the unlike interaction

Viscosity and thermal conductivity values obtained for the (CH_4 + CO_2) and (CH_4 + H_2S) systems using the unadjusted PESs for the unlike interactions differ by no more than +0.4% and +0.3%, respectively, from those obtained using the adjusted PESs at any temperature or composition. The relative deviations of viscosity and thermal conductivity values obtained for the (H_2S + CO_2) system using the modified H_2S–CO_2 PES (see Section 4.1.3) from those obtained using the unmodified one are less than +0.2%. In the case of the binary diffusion coefficient, the corresponding deviations do not exceed +0.9%, +0.8%, and +0.4% for the (CH_4 + CO_2), (CH_4 + H_2S), and (H_2S + CO_2) systems, respectively. The reason for the larger relative deviations, compared with the other two transport properties, is that the binary diffusion coefficient in the first-order approximation is determined solely by the potential for the unlike interaction. As a consequence, it is independent of composition. Generalized cross sections for the like interactions only enter into higher-order approximations, resulting in a weak composition dependence.

4.2.3. Comparison with experimental data

For the comparison with experimental shear viscosity data in the dilute gas limit for the (CH_4 + CO_2) system, we use the values computed using the adjusted CH_4–CO_2 PES and the CH_4–CH_4 and CO_2–CO_2 PESs of Refs. [3] and [5]. In figure 6, the calculated viscosity values are compared with the experimental data of Kestin and co-workers for the mixture [60, 61] and the experimental data of Vogel for the pure components [62, 63]. We have not included the recent mixture data of Locke et al. [64] in the comparison because the densities at which these measurements were carried out are too high for a reliable extrapolation to the dilute gas limit. The data of Vogel, which extend from ambient temperature up to almost 700 K, are of reference quality, with expanded (k = 2) uncertainties of less than 0.4%. The deviations from the calculated values are nearly independent of temperature and are on average +0.55% for carbon dioxide and −0.45% for methane. It was therefore suggested [5, 14] that the best viscosity values for the two pure species over a wide temperature range are obtained by scaling the computed viscosity values for carbon dioxide by a factor of 1.0055 and those for methane by a factor of 0.9955 at all temperatures. In Ref. [14], we proposed a viscosity scaling factor for (CH_4 + N_2) mixtures that depends linearly on composition and reproduces the optimal scaling factors for the two pure components. Following this approach, we obtain for (CH_4 + CO_2) mixtures

$$\eta_{\mathrm{rec}} = \eta_{\mathrm{calc}} \left(1.0055 x_{\mathrm{CO_2}} + 0.9955 x_{\mathrm{CH_4}}\right), \tag{12}$$

where η_{calc} are the calculated values and η_{rec} the recommended ones. As can be seen in figure 6, the data of Kestin and co-workers [60, 61] between (293 and 303) K are in excellent agreement with the recommended values, whereas the data of Kestin and Ro at higher temperatures show larger deviations of up to +1.2%, despite a claimed uncertainty of only 0.3%. However, it has been established [65] that the viscometer used by Kestin and Ro suffered from a design flaw concerning the temperature measurement, which resulted in viscosity values that are systematically too high above room temperature. The data of Kestin and Ro for the (CH_4 + N_2) system [61], which were measured using the same viscometer, show a similar behavior in comparison with our calculated and recommended values [14].

Figure 7 shows the comparison of the thermal conductivity values (calculated using the same PESs as for viscosity) with the available experimental data for dilute (CH_4 + CO_2) mixtures [66–69]. The room temperature data of Kestin et al. [67], which were measured by means of the transient hot-wire (THW) technique, differ by only +(0.3 to 0.8)% from the calculated values. Kestin et al. did not provide an uncertainty estimate for their data, but a value of 0.3% is given for thermal conductivity measurements of (CH_4 + N_2) mixtures [70] obtained in the same THW apparatus. Pátek et al. [69] also performed measurements of the thermal conductivity of (CH_4 + CO_2) mixtures using the THW technique, but in an extended temperature range of (300 to 425) K. The relative deviations between the measured and calculated values increase with temperature from about +1% at 300 K up to about +(4 to 5)% at (400 and 425) K. The trend and magnitude of the deviations are similar to those observed for (CH_4 + N_2) mixtures [14], which were investigated by Pátek and co-workers using the same instrument [71]. Although, Pátek et al. claimed an expanded uncertainty (95% confidence level) of 1.2% for their data [69], there is growing circumstantial evidence that measurements by means of the THW technique at low densities and at temperatures higher than ambient suffer

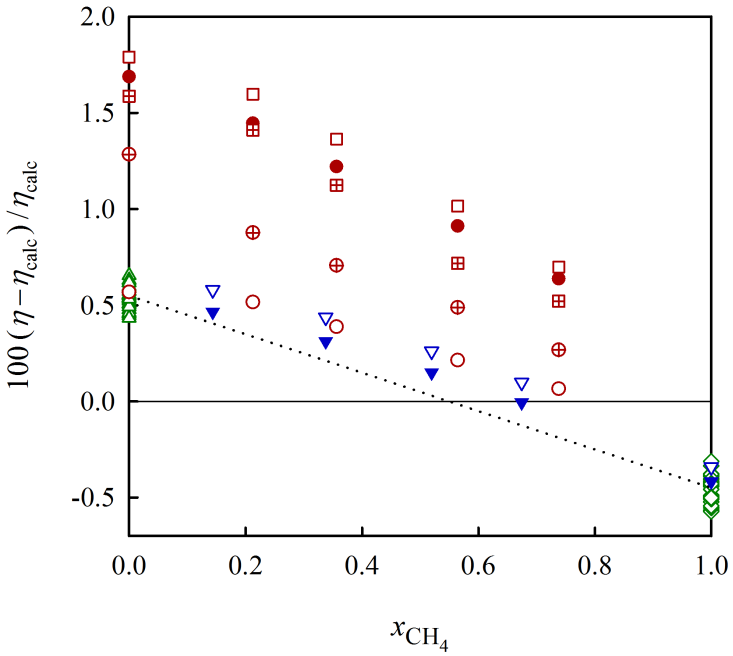

Figure 6: Relative deviations of experimental data for the dilute gas viscosity of (CH_4 + CO_2) mixtures and the pure components from values calculated using the adjusted CH_4–CO_2 potential function of the present work, the CH_4–CH_4 potential function of Ref. [3], and the CO_2–CO_2 potential function of Ref. [5] as a function of methane mole fraction: ▼, Kestin and Yata [60], 293 K; ▽, Kestin and Yata [60], 303 K; ○, Kestin and Ro [61], 298 K; ⊕, Kestin and Ro [61], 323 K; ●, Kestin and Ro [61], 373 K; □, Kestin and Ro [61], 423 K; ⊞, Kestin and Ro [61], 473 K; ◇, Vogel [62], (292 to 682) K; △, Vogel [63], (298 to 683) K. The dotted line indicates the recommended values resulting from Equation (12).

from a systematic error [14, 72, 73]. Figure 7 also includes the deviations of the data of Rosenbaum and Thodos [66] and of Yorizane et al. [68], which do not exceed −8.6% and −6.0%, respectively. The relative deviations do not exhibit any systematic temperature or composition trends, but are larger than the claimed uncertainty of 3% given by the authors [66, 68]. The magnitude of the deviations is not surprising as the pure species data of Rosenbaum and Thodos [66] exhibit similar deviations, while the data of Yorizane et al. [68], which were measured at temperatures of (298 and 308) K, deviate by as much as 6% from those of Kestin et al. [67]. The most reliable experimental data for pure carbon dioxide are probably those of Haarman [74] (also depicted in Figure 7), which deviate from the computed values on average by +1.1%. A scaling of the computed values by a factor of 1.011 at all temperatures was therefore recommended [5]. For pure methane, we do not propose a scaling of the calculated thermal conductivity values because the agreement with the best experimental data, see Ref. [10], is highly satisfactory even without scaling. In analogy to Equation (12), the recommended scaling procedure for (CH_4 + CO_2) mixtures is then given by

$$\lambda_{\mathrm{rec}} = \lambda_{\mathrm{calc}} \left(1.011 x_{\mathrm{CO_2}} + x_{\mathrm{CH_4}}\right). \tag{13}$$

Unfortunately, there appear to be no experimental data for the binary diffusion coefficient of the (CH_4 + CO_2) system with which to compare the present results.

We could not find any experimental data on the transport properties of (CH_4 + H_2S) and (H_2S + CO_2) gas mixtures in the literature. For pure hydrogen sulfide, our calculated viscosity values agree exceptionally well with the reference data of Vogel [62] for the temperature range from (292 to 682) K. His data differ on average by only −0.1% (with a maximum deviation of −0.16%), so that a scaling of the calculated viscosity values by a factor of 0.999 is appropriate. Thus, our recommended viscosity values for the (CH_4 + H_2S) and (H_2S + CO_2) systems are given as

$$\eta_{\mathrm{rec}} = \eta_{\mathrm{calc}} \left(0.9955 x_{\mathrm{CH_4}} + 0.999 x_{\mathrm{H_2S}}\right), \tag{14}$$

and

$$\eta_{\mathrm{rec}} = \eta_{\mathrm{calc}} \left(0.999 x_{\mathrm{H_2S}} + 1.0055 x_{\mathrm{CO_2}}\right), \tag{15}$$

respectively. Due to the scarcity of accurate thermal conductivity data for pure hydrogen sulfide, see Refs. [4] and [12], a scaling factor for the corresponding calculated values cannot be determined reliably, so that we do not propose a scaling of the thermal conductivity values for pure hydrogen sulfide. Thus, for the (CH_4 + H_2S) and (H_2S + CO_2) systems, we have $\lambda_{\mathrm{rec}} = \lambda_{\mathrm{calc}}$ and

$$\lambda_{\mathrm{rec}} = \lambda_{\mathrm{calc}} \left(x_{\mathrm{H_2S}} + 1.011 x_{\mathrm{CO_2}}\right), \tag{16}$$

respectively.

Our estimates for the relative combined expanded ($k = 2$) uncertainties of the calculated transport property values listed in Tables 3–6 are given in the table footnotes. If a scaling is recommended, the uncertainty estimates refer to the scaled values.

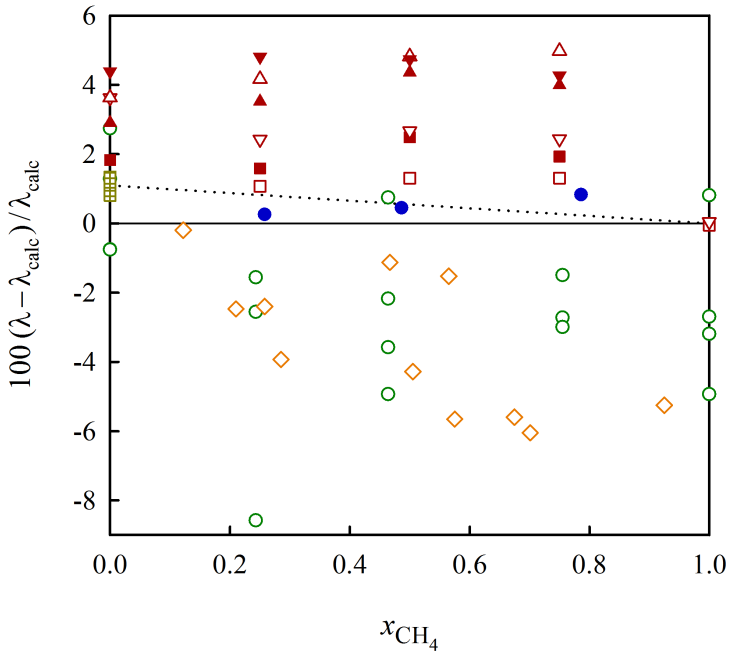

Figure 7: Relative deviations of experimental data for the dilute gas thermal conductivity of (CH_4 + CO_2) mixtures and the pure components from values calculated using the adjusted CH_4–CO_2 potential function of the present work, the CH_4–CH_4 potential function of Ref. [3], and the CO_2–CO_2 potential function of Ref. [5] as a function of methane mole fraction: ○, Rosenbaum and Thodos [66], (335 to 435) K; ⊞, Haarman [74], (328 to 468) K; ●, Kestin et al. [67], 301 K; ◇, Yorizane et al. [68], (298 and 308) K; □, Pátek and Klomfar [75] and Pátek et al. [69], 300 K; ■, Pátek et al. [69], 325 K; ▽, Pátek and Klomfar [75] and Pátek et al. [69], 350 K; ▲, Pátek et al. [69], 375 K; △, Pátek et al. [69], 400 K; ▼, Pátek et al. [69], 425 K. The dotted line indicates the recommended values resulting from Equation (13).

5. Summary and conclusions

New intermolecular potential energy surfaces for the CH_4–CO_2, CH_4–H_2S, and H_2S–CO_2 molecule pairs were determined from quantum-chemical *ab initio* calculations. The CH_4, CO_2, and H_2S molecules were treated as rigid rotors in their zero-point vibrationally averaged geometries in the *ab initio* calculations. The potential energy surfaces are represented by accurate analytical site-site potential functions using the positions and partial charges of the sites obtained in our previous work on the pure species. Since zero-point vibrational effects (which are particularly important for interactions involving methane) are only partly accounted for in our approach, small empirical adjustments of the CH_4–CO_2 and CH_4–H_2S potential functions were performed utilizing the most accurate experimental data for the cross second virial coefficient of the CH_4–CO_2 molecule pair.

The new potential energy surfaces and the already available ones for the CH_4–CH_4, CO_2–CO_2, and H_2S–H_2S interactions [3–5] were used to calculate the cross second virial coefficients as well as the dilute gas shear viscosities, thermal conductivities, and binary diffusion coefficients of (CH_4 + CO_2), (CH_4 + H_2S), and (H_2S + CO_2) mixtures. The cross second virial coefficients were computed by means of the Mayer-sampling Monte Carlo approach [22]. To account for quantum effects, the quadratic Feynman–Hibbs effective pair potential [23] was used in these calculations. The transport properties were calculated using the classical trajectory method in conjunction with the kinetic theory of molecular gases [8, 14, 24–26]. The viscosity and thermal conductivity values computed using the unadjusted potentials for the unlike interactions differ by no more than +0.4%, while the binary diffusion coefficients differ by no more than +0.9% from those obtained using the adjusted potentials.

The calculated values for the cross second virial coefficient of the (CH_4 + CO_2) system agree with the available experimental data to better than ±5 $cm^3 \cdot mol^{-1}$. For (CH_4 + H_2S) and (H_2S + CO_2) gas mixtures, only one set of virial measurements each is available for the analysis, and although acceptable agreement is achieved, it is insufficient to fully validate the developed potential functions. Transport property data for the three mixtures are scant; data exist only for the viscosity and thermal conductivity of (CH_4 + CO_2) mixtures. Close to room temperature, the agreement with the calculated values is good, nearly within the claimed uncertainty of the experimental data. At temperatures higher than ambient, the known issues [14, 65, 72, 73] with both the viscometer employed and the transient hot-wire method do not allow for a meaningful comparison.

Tables of recommended values for all investigated thermophysical properties in the temperature range from (150 to 1200) K and, in the case of the transport properties, for a number of mixture compositions are provided. Estimates of combined expanded uncertainties with a confidence level of approximately 95% are also provided for each property of each mixture. Furthermore, simple correlations for the cross second virial coefficients as a function of temperature were developed. Our recommended values represent the most accurate estimates to date for the cross second virial coefficients and dilute gas transport properties of the (CH_4 + CO_2), (CH_4 + H_2S), and (H_2S + CO_2) systems.

Acknowledgment

This work was financially supported by the Deutsche Forschungsgemeinschaft (DFG), Grant Nos. HE 6155/1-1 and BI 1389/1-1.

Appendix A. Supplementary data

Supplementary data associated with this article can be found, in the online version, at http://dx.doi.org/10.1016/j.jct.2016.07.034.

References

[1] E. Hendriks, G. M. Kontogeorgis, R. Dohrn, J.-C. de Hemptinne, I. G. Economou, L. F. Zilnik, V. Vesovic, Ind. Eng. Chem. Res. 49 (2010) 11131–11141.

[2] M. J. Assael, A. R. H. Goodwin, V. Vesovic, W. A. Wakeham (Eds.), Experimental Thermodynamics Volume IX: Advances in Transport Properties of Fluids, The Royal Society of Chemistry, Cambridge, 2014.

[3] R. Hellmann, E. Bich, E. Vogel, J. Chem. Phys. 128 (2008) 214303.

[4] R. Hellmann, E. Bich, E. Vogel, V. Vesovic, Phys. Chem. Chem. Phys. 13 (2011) 13749–13758.

[5] R. Hellmann, Chem. Phys. Lett. 613 (2014) 133–138.

[6] J.-P. Crusius, R. Hellmann, E. Hassel, E. Bich, J. Chem. Phys. 141 (2014) 164322.

[7] R. Hellmann, J. B. Mehl, V. Vesovic, in: M. J. Assael, A. R. H. Goodwin, V. Vesovic, W. A. Wakeham (Eds.), Experimental Thermodynamics Volume IX: Advances in Transport Properties of Fluids, The Royal Society of Chemistry, Cambridge, 2014, pp. 234–252.

[8] R. Hellmann, E. Bich, V. Vesovic, J. Chem. Phys. 144 (2016) 134301.

[9] R. Hellmann, E. Bich, E. Vogel, A. S. Dickinson, V. Vesovic, J. Chem. Phys. 129 (2008) 064302.

[10] R. Hellmann, E. Bich, E. Vogel, A. S. Dickinson, V. Vesovic, J. Chem. Phys. 130 (2009) 124309.

[11] R. Hellmann, E. Bich, E. Vogel, V. Vesovic, J. Chem. Eng. Data 57 (2012) 1312–1317.

[12] R. Hellmann, E. Bich, Mol. Phys. 113 (2015) 176–183.

[13] R. Hellmann, E. Vogel, J. Chem. Eng. Data 60 (2015) 3600–3605.

[14] R. Hellmann, E. Bich, E. Vogel, V. Vesovic, J. Chem. Phys. 141 (2014) 224301.

[15] World Energy Outlook – Are we entering a golden age of gas?, Report, International Energy Agency, Paris, 2011.

[16] A. J. Kidnay, W. R. Parrish, D. G. McCartney, Fundamentals of Natural Gas Processing, 2nd ed., CRC Press, Taylor & Francis Group, Boca Raton, 2011.

[17] A. F. Ismail, K. Khulbe, T. Matsuura, Gas Separation Membranes, Springer International Publishing, Switzerland, 2015.

[18] M. T. Oakley, H. Do, R. J. Wheatley, Fluid Phase Equilib. 290 (2010) 48–54.

[19] S. J. Pai, Y. C. Bae, J. Chem. Phys. 141 (2014) 064303.

[20] K. Raghavachari, G. W. Trucks, J. A. Pople, M. Head-Gordon, Chem. Phys. Lett. 157 (1989) 479–483.

[21] D. E. Woon, P. Zeng, D. R. Beck, J. Chem. Phys. 93 (1990) 7808–7812.

[22] J. K. Singh, D. A. Kofke, Phys. Rev. Lett. 92 (2004) 220601.

[23] R. P. Feynman, A. R. Hibbs, Quantum Mechanics and Path Integrals, McGraw-Hill, New York, 1965.

[24] F. R. W. McCourt, J. J. M. Beenakker, W. E. Köhler, I. Kuščer, Nonequilibrium Phenomena in Polyatomic Gases, volume I: Dilute Gases, Clarendon Press, Oxford, 1990.

[25] E. L. Heck, A. S. Dickinson, Comput. Phys. Commun. 95 (1996) 190–220.

[26] A. S. Dickinson, R. Hellmann, E. Bich, E. Vogel, Phys. Chem. Chem. Phys. 9 (2007) 2836–2843.

[27] S. F. Boys, F. Bernardi, Mol. Phys. 19 (1970) 553–566.

[28] T. H. Dunning, Jr., J. Chem. Phys. 90 (1989) 1007–1023.

[29] R. A. Kendall, T. H. Dunning, Jr., R. J. Harrison, J. Chem. Phys. 96 (1992) 6796–6806.

[30] T. H. Dunning, Jr., K. A. Peterson, A. K. Wilson, J. Chem. Phys. 114 (2001) 9244–9253.

[31] A. Halkier, T. Helgaker, P. Jørgensen, W. Klopper, H. Koch, J. Olsen, A. K. Wilson, Chem. Phys. Lett. 286 (1998) 243–252.

[32] CFOUR, Coupled-Cluster techniques for Computational Chemistry, a quantum-chemical program package by J. F. Stanton, J. Gauss, M. E. Harding, P. G. Szalay with contributions from A. A. Auer, R. J. Bartlett, U. Benedikt, C. Berger, D. E. Bernholdt, Y. J. Bomble, L. Cheng, O. Christiansen, M. Heckert, O. Heun, C. Huber, T.-C. Jagau, D. Jonsson, J. Jusélius, K. Klein, W. J. Lauderdale, D. A. Matthews, T. Metzroth, L. A. Mück, D. P. O'Neill, D. R. Price, E. Prochnow, C. Puzzarini, K. Ruud, F. Schiffmann, W. Schwalbach, S. Stopkowicz, A. Tajti, J. Vázquez, F. Wang, J. D. Watts and the integral packages MOLECULE (J. Almlöf and P. R. Taylor), PROPS (P. R. Taylor), ABACUS (T. Helgaker, H. J. Aa. Jensen, P. Jørgensen, and J. Olsen), and ECP routines by A. V. Mitin and C. van Wüllen. For the current version, see http://www.cfour.de.

[33] K. T. Tang, J. P. Toennies, J. Chem. Phys. 80 (1984) 3726–3741.

[34] A. J. Russell, M. A. Spackman, Mol. Phys. 84 (1995) 1239–1255.

[35] D. M. Bishop, F. L. Gu, S. M. Cybulski, J. Chem. Phys. 109 (1998) 8407–8415.

[36] S. M. Cybulski, T. P. Haley, J. Chem. Phys. 121 (2004) 7711–7716.

[37] B. Jäger, R. Hellmann, E. Bich, E. Vogel, J. Chem. Phys. 135 (2011) 084308.

[38] L. Waldmann, in: S. Flügge (Ed.), Handbuch der Physik, volume 12, Springer-Verlag, Berlin, 1958, pp. 295–514.

[39] L. Waldmann, E. Trübenbacher, Z. Naturforsch. A 17 (1962) 363–376.

[40] J. H. Ferziger, H. G. Kaper, The Mathematical Theory of Transport Processes in Gases, North-Holland, Amsterdam, 1972.

[41] C. F. Curtiss, J. Chem. Phys. 75 (1981) 1341–1346.

[42] M. Mustafa, Measurement and Calculation of Transport Properties of Polyatomic Gases, Ph.D. thesis, Imperial College London, London, UK, 1987.

[43] E. L. Heck, A. S. Dickinson, Physica A 217 (1995) 107–123.

[44] U. Setzmann, W. Wagner, J. Phys. Chem. Ref. Data 20 (1991) 1061–1155.

[45] R. Span, W. Wagner, J. Phys. Chem. Ref. Data 25 (1996) 1509–1596.

[46] E. W. Lemmon, R. Span, J. Chem. Eng. Data 51 (2006) 785–850.

[47] J. Brewer, Determination of mixed virial coefficients, Technical Report, AFOSR No. 67-2795, 1967.

[48] H.-J. Ng, Interaction Virial Coefficients in Binary Mixtures of Methane, Nitrogen and Carbon Dioxide, Master's thesis, University of Alberta, Edmonton, Alberta, Canada, 1971.

[49] T. Katayama, K. Ohgaki, H. Ohmori, J. Chem. Eng. Jpn. 13 (1980) 257–262.

[50] K. Ohgaki, Y. Nakamura, H. Ariyasu, T. Katayama, J. Chem. Eng. Jpn. 15 (1982) 85–90.

[51] M. L. Martin, R. D. Trengove, K. R. Harris, P. J. Dunlop, Aust. J. Chem. 35 (1982) 1525–1529.

[52] M. Jaeschke, S. Audibert, P. van Caneghem, A. E. Humphreys, R. Janssen-van Rosmalen, Q. Pellei, J. P. J. Michels, J. A. Schouten, C. A. ten Seldam, GERG Tech. Monogr. TM2, 1988.

[53] G. J. Esper, D. M. Bailey, J. C. Holste, K. R. Hall, Fluid Phase Equilib. 49 (1989) 35–47.

[54] P. J. McElroy, L. L. Kee, C. A. Renner, J. Chem. Eng. Data 35 (1990) 314–317.

[55] B. V. Mallu, D. S. Viswanath, J. Chem. Thermodyn. 22 (1990) 997–1006.

[56] G. A. Iglesias-Silva, M. S. Mannan, F. Y. Shaikh, K. R. Hall, Fluid Phase Equilib. 161 (1999) 33–43.

[57] J. H. Dymond, K. N. Marsh, R. C. Wilhoit, in: M. Frenkel, K. N. Marsh (Eds.), Landolt-Börnstein: Numerical Data and Functional Relationships in Science and Technology: New Series, volume 21B: Virial Coefficients of Mixtures of *Group IV: Physical Chemistry*, Springer, Berlin–Heidelberg–New York, 2002, p. 85.

[58] D. M. Bailey, C. H. Liu, J. C. Holste, K. R. Hall, P. T. Eubank, K. N. Marsh, Thermodynamic Properties of Pure Hydrogen Sulfide and Mixtures Containing Hydrogen Sulfide with Methane, Carbon Dioxide, Methylcyclohexane and Toluene, GPA Research Report 107, Gas

Processors Association, Tulsa, USA, 1987.

[59] C. E. Stouffer, S. J. Kellerman, K. R. Hall, J. C. Holste, B. E. Gammon, K. N. Marsh, J. Chem. Eng. Data 46 (2001) 1309–1318.

[60] J. Kestin, J. Yata, J. Chem. Phys. 49 (1968) 4780–4791.

[61] J. Kestin, S. T. Ro, Ber. Bunsenges. Phys. Chem. 78 (1974) 20–24.

[62] E. Vogel, J. Chem. Eng. Data 56 (2011) 3265–3272.

[63] E. Vogel, Int. J. Thermophys. 37 (2016) 63.

[64] C. R. Locke, P. L. Stanwix, T. J. Hughes, M. L. Johns, A. R. H. Goodwin, K. N. Marsh, G. Galliero, E. F. May, J. Chem. Thermodyn. 87 (2015) 162–167.

[65] E. Vogel, C. Küchenmeister, E. Bich, A. Laesecke, J. Phys. Chem. Ref. Data 27 (1998) 947–970.

[66] B. M. Rosenbaum, G. Thodos, J. Chem. Phys. 51 (1969) 1361–1368.

[67] J. Kestin, S. T. Ro, Y. Nagasaka, Ber. Bunsenges. Phys. Chem. 86 (1982) 945–948.

[68] M. Yorizane, S. Yoshimura, H. Masuoka, H. Yoshida, Ind. Eng. Chem. Fundamen. 22 (1983) 458–463.

[69] J. Pátek, J. Klomfar, L. Čapla, P. Buryan, Int. J. Thermophys. 26 (2005) 577–592.

[70] J. Kestin, Y. Nagasaka, W. A. Wakeham, Ber. Bunsenges. Phys. Chem. 86 (1982) 632–636.

[71] J. Pátek, J. Klomfar, L. Čapla, P. Buryan, Int. J. Thermophys. 24 (2003) 923–935.

[72] S. H. Jawad, Thermal conductivity of polyatomic gases, Ph.D. thesis, Imperial College London, 1999.

[73] W. A. Wakeham, in: D. S. Gaal (Ed.), Proceedings of the 30th International Thermal Conductivity Conference and the 18th International Thermal Expansion Symposium, DEStech Publications, Lancaster, PA, 2010, pp. 14–37.

[74] J. W. Haarman, Am. Inst. Phys. Conf. Proc. 11 (1973) 193–198.

[75] J. Pátek, J. Klomfar, Fluid Phase Equilib. 198 (2002) 147–163.

Table 1: Calculated semiclassical values, B_{12}^{QFH}, for the cross second virial coefficients of the CH_4–CO_2, CH_4–H_2S, and H_2S–CO_2 molecule pairs and their combined expanded ($k = 2$) uncertainties, U_c, as a function of temperature.[a]

T/K	$CH_4 - CO_2$		$CH_4 - H_2S$		$H_2S - CO_2$	
	$B_{12}^{\mathrm{QFH}}/(\mathrm{cm^3 \cdot mol^{-1}})$	$U_c/(\mathrm{cm^3 \cdot mol^{-1}})$	$B_{12}^{\mathrm{QFH}}/(\mathrm{cm^3 \cdot mol^{-1}})$	$U_c/(\mathrm{cm^3 \cdot mol^{-1}})$	$B_{12}^{\mathrm{QFH}}/(\mathrm{cm^3 \cdot mol^{-1}})$	$U_c/(\mathrm{cm^3 \cdot mol^{-1}})$
150	−268.2	4.9	−280.7	13.4	−705.3	36.2
160	−235.1	4.2	−248.3	11.7	−585.8	28.0
170	−208.1	3.7	−221.5	10.4	−496.5	22.3
180	−185.7	3.3	−198.9	9.4	−427.8	18.3
190	−166.7	3.0	−179.7	8.5	−373.4	15.3
200	−150.4	2.7	−163.2	7.8	−329.5	13.0
210	−136.4	2.5	−148.8	7.2	−293.4	11.2
220	−124.1	2.3	−136.2	6.7	−263.2	9.8
230	−113.3	2.1	−125.1	6.2	−237.7	8.7
240	−103.8	2.0	−115.1	5.8	−215.9	7.8
250	−95.22	1.8	−106.2	5.5	−196.9	7.0
260	−87.55	1.7	−98.23	5.2	−180.4	6.4
270	−80.62	1.6	−90.99	4.9	−165.9	5.8
273.15	−78.58	1.6	−88.85	4.8	−161.7	5.7
280	−74.35	1.5	−84.40	4.6	−153.0	5.4
290	−68.63	1.5	−78.39	4.4	−141.5	5.0
298.15	−64.33	1.5	−73.87	4.2	−133.0	4.7
300	−63.40	1.5	−72.89	4.2	−131.2	4.6
310	−58.60	1.5	−67.82	4.0	−121.9	4.3
320	−54.18	1.5	−63.16	3.8	−113.5	4.0
330	−50.09	1.5	−58.84	3.7	−105.8	3.8
340	−46.31	1.5	−54.83	3.5	−98.79	3.6
350	−42.80	1.5	−51.10	3.4	−92.35	3.4
360	−39.53	1.5	−47.63	3.3	−86.43	3.2
370	−36.48	1.5	−44.39	3.2	−80.96	3.1
380	−33.62	1.5	−41.35	3.1	−75.90	2.9
390	−30.95	1.5	−38.50	3.0	−71.20	2.8
400	−28.43	1.5	−35.83	2.9	−66.83	2.7
420	−23.85	1.5	−30.93	2.7	−58.94	2.5
440	−19.76	1.5	−26.57	2.6	−52.01	2.3
460	−16.10	1.5	−22.65	2.4	−45.88	2.2
480	−12.81	1.5	−19.13	2.3	−40.43	2.0
500	−9.83	1.5	−15.93	2.2	−35.55	1.9
520	−7.12	1.5	−13.03	2.1	−31.16	1.8
540	−4.66	1.5	−10.38	2.0	−27.18	1.7
560	−2.40	1.5	−7.95	1.9	−23.57	1.7
580	−0.32	1.5	−5.72	1.9	−20.28	1.6
600	1.59	1.5	−3.66	1.8	−17.27	1.5
650	5.76	1.5	0.83	1.7	−10.74	1.5
700	9.23	1.5	4.57	1.5	−5.37	1.5
750	12.15	1.5	7.73	1.5	−0.89	1.5
800	14.64	1.5	10.42	1.5	2.91	1.5
900	18.65	1.5	14.76	1.5	8.97	1.5
1000	21.70	1.5	18.07	1.5	13.56	1.5
1100	24.09	1.5	20.67	1.5	17.14	1.5
1200	25.99	1.5	22.74	1.5	19.99	1.5

[a] The values for the CH_4–CO_2 and CH_4–H_2S molecule pairs were obtained using the adjusted potential functions.

Table 2: Coefficients of the function fitted to the calculated semiclassical values for the cross second virial coefficient (Equation (11)).[a]

Molecule pair	b_0	$b_{0.5}$	b_1	b_2	b_3	b_4	b_5	b_6
$CH_4 - CO_2$	2.5460×10^1	1.4712×10^2	-5.0983×10^2	1.2350×10^2	-5.7429×10^2	3.8868×10^2	-2.6857×10^2	
$CH_4 - H_2S$	2.2871×10^1	1.5545×10^2	-5.4696×10^2	1.2751×10^2	-5.7098×10^2	3.7859×10^2	-2.1400×10^2	
$H_2S - CO_2$	2.8016×10^1	1.4001×10^2	-5.5415×10^2	-3.1652×10^2	8.5273×10^1	-2.6443×10^3	3.3173×10^3	-3.1580×10^3

[a] The coefficients for the CH_4–CO_2 and CH_4–H_2S molecule pairs were obtained by fitting to the values resulting from the adjusted potential functions.

Table 3: Calculated values for the shear viscosity, η, and the thermal conductivity, λ, of the pure gases methane, carbon dioxide, and hydrogen sulfide in the dilute gas limit as a function of temperature.

T/K	CH_4		CO_2		H_2S	
	$\eta/(\mu\text{Pa}\cdot\text{s})$ [a]	$\lambda/(\text{mW}\cdot\text{m}^{-1}\cdot\text{K}^{-1})$ [b]	$\eta/(\mu\text{Pa}\cdot\text{s})$ [c]	$\lambda/(\text{mW}\cdot\text{m}^{-1}\cdot\text{K}^{-1})$ [d]	$\eta/(\mu\text{Pa}\cdot\text{s})$ [e]	$\lambda/(\text{mW}\cdot\text{m}^{-1}\cdot\text{K}^{-1})$ [f]
150	5.820	16.04	7.687	6.659	6.135	6.738
175	6.778	18.89	8.880	7.978	7.087	7.862
200	7.715	21.77	10.09	9.449	8.069	9.030
225	8.627	24.70	11.30	11.05	9.077	10.25
250	9.511	27.75	12.51	12.77	10.11	11.53
273.15	10.30	30.72	13.63	14.44	11.07	12.77
298.15	11.13	34.11	14.82	16.31	12.12	14.16
325	12.00	37.98	16.09	18.38	13.25	15.72
350	12.77	41.81	17.25	20.35	14.29	17.22
375	13.52	45.84	18.39	22.35	15.33	18.78
400	14.25	50.06	19.52	24.36	16.36	20.37
425	14.96	54.46	20.61	26.39	17.37	22.00
450	15.65	59.01	21.69	28.42	18.37	23.67
475	16.33	63.70	22.75	30.46	19.35	25.36
500	16.98	68.52	23.78	32.49	20.32	27.09
550	18.25	78.46	25.79	36.53	22.20	30.61
600	19.47	88.76	27.71	40.54	24.02	34.23
650	20.64	99.33	29.56	44.49	25.77	37.92
700	21.78	110.1	31.35	48.37	27.47	41.69
750	22.87	121.1	33.07	52.19	29.11	45.50
800	23.94	132.1	34.74	55.93	30.71	49.35
900	25.99	154.5	37.93	63.20	33.76	57.11
1000	27.94	177.0	40.95	70.15	36.66	64.87
1100	29.82	199.3	43.83	76.82	39.42	72.56
1200	31.64	221.4	46.58	83.21	42.07	80.14

[a] Viscosity values for CH_4 taken from Ref. [14]. These values should be scaled by a factor of 0.9955 to obtain the recommended values. The relative combined expanded ($k = 2$) uncertainty of the scaled values is 0.4% for $300 \leqslant T/\text{K} \leqslant 700$, 0.8% for $200 \leqslant T/\text{K} < 300$ and $700 < T/\text{K} \leqslant 1000$, and 1.2% for $150 \leqslant T/\text{K} < 200$ and $1000 < T/\text{K} \leqslant 1200$.

[b] Thermal conductivity values for CH_4 taken from Ref. [8]. The relative combined expanded ($k = 2$) uncertainty of these values is 1.0% for $300 \leqslant T/\text{K} \leqslant 700$, 1.5% for $200 \leqslant T/\text{K} < 300$ and $700 < T/\text{K} \leqslant 1000$, and 2.0% for $150 \leqslant T/\text{K} < 200$ and $1000 < T/\text{K} \leqslant 1200$.

[c] Viscosity values for CO_2 taken from Ref. [5]. These values should be scaled by a factor of 1.0055 to obtain the recommended values. The relative combined expanded ($k = 2$) uncertainty of the scaled values is 0.4% for $300 \leqslant T/\text{K} \leqslant 700$, 0.8% for $200 \leqslant T/\text{K} < 300$ and $700 < T/\text{K} \leqslant 1200$, and 2.0% for $150 \leqslant T/\text{K} < 200$.

[d] Thermal conductivity values for CO_2 taken from Ref. [5]. These values should be scaled by a factor of 1.011 to obtain the recommended values. The relative combined expanded ($k = 2$) uncertainty of the scaled values is 1.0% for $300 \leqslant T/\text{K} \leqslant 700$, 1.5% for $200 \leqslant T/\text{K} < 300$ and $700 < T/\text{K} \leqslant 1200$, and 2.0% for $150 \leqslant T/\text{K} < 200$.

[e] Previously unpublished viscosity values for H_2S. Some of the values coincide with values from Ref. [11] due to rounding. The values should be scaled by a factor of 0.999 to obtain the recommended values. The relative combined expanded ($k = 2$) uncertainty of the scaled values is 0.6% for $300 \leqslant T/\text{K} \leqslant 700$, 1.0% for $200 \leqslant T/\text{K} < 300$ and $700 < T/\text{K} \leqslant 1200$, and 2.0% for $150 \leqslant T/\text{K} < 200$.

[f] Previously unpublished thermal conductivity values for H_2S at (150, 175, 273.15, 298.15, 425, and 475) K; other values taken from Ref. [12]. The relative combined expanded ($k = 2$) uncertainty of these values is 1.5% for $300 \leqslant T/\text{K} \leqslant 700$, 2.0% for $200 \leqslant T/\text{K} < 300$ and $700 < T/\text{K} \leqslant 1200$, and 3.0% for $150 \leqslant T/\text{K} < 200$.

Table 4: Calculated values for the shear viscosity, η, of (CH_4 + CO_2), (CH_4 + H_2S), and (H_2S + CO_2) mixtures in the dilute gas limit as a function of mole fraction and temperature.[a]

T/K	η/(μPa·s)											
	CH_4 (1) + CO_2 (2)				CH_4 (1) + H_2S (2)				H_2S (1) + CO_2 (2)			
	x_1 = 0.2	x_1 = 0.4	x_1 = 0.6	x_1 = 0.8	x_1 = 0.2	x_1 = 0.4	x_1 = 0.6	x_1 = 0.8	x_1 = 0.2	x_1 = 0.4	x_1 = 0.6	x_1 = 0.8
150	7.499	7.242	6.896	6.433	6.179	6.187	6.145	6.031	7.413	7.119	6.808	6.479
175	8.685	8.406	8.020	7.491	7.159	7.185	7.149	7.025	8.584	8.255	7.895	7.505
200	9.876	9.570	9.136	8.535	8.158	8.194	8.154	8.008	9.775	9.416	9.011	8.561
225	11.07	10.72	10.24	9.558	9.173	9.206	9.151	8.974	10.98	10.59	10.15	9.641
250	12.25	11.86	11.32	10.55	10.20	10.22	10.14	9.918	12.18	11.78	11.29	10.74
273.15	13.33	12.90	12.29	11.45	11.15	11.15	11.03	10.77	13.30	12.87	12.36	11.76
298.15	14.49	14.00	13.33	12.40	12.18	12.14	11.99	11.67	14.49	14.05	13.51	12.86
325	15.71	15.16	14.40	13.38	13.27	13.19	12.99	12.61	15.75	15.30	14.73	14.04
350	16.82	16.21	15.38	14.26	14.28	14.16	13.90	13.45	16.91	16.44	15.85	15.13
375	17.91	17.24	16.33	15.12	15.27	15.10	14.79	14.28	18.05	17.57	16.95	16.21
400	18.98	18.24	17.26	15.96	16.25	16.03	15.66	15.08	19.16	18.67	18.04	17.27
425	20.02	19.22	18.16	16.77	17.22	16.94	16.50	15.86	20.25	19.75	19.10	18.31
450	21.04	20.18	19.04	17.56	18.17	17.83	17.33	16.63	21.32	20.81	20.15	19.33
475	22.04	21.11	19.90	18.34	19.10	18.71	18.14	17.37	22.37	21.85	21.17	20.34
500	23.02	22.02	20.74	19.09	20.01	19.56	18.94	18.10	23.40	22.86	22.17	21.33
550	24.91	23.79	22.36	20.54	21.79	21.22	20.47	19.50	25.39	24.83	24.12	23.24
600	26.73	25.48	23.91	21.94	23.50	22.82	21.95	20.85	27.29	26.72	25.98	25.09
650	28.47	27.11	25.40	23.28	25.15	24.36	23.37	22.15	29.13	28.53	27.78	26.86
700	30.15	28.67	26.84	24.57	26.74	25.84	24.74	23.40	30.89	30.28	29.51	28.58
750	31.78	30.19	28.23	25.83	28.28	27.28	26.07	24.61	32.60	31.97	31.18	30.23
800	33.35	31.66	29.58	27.04	29.78	28.67	27.36	25.79	34.25	33.60	32.80	31.84
900	36.36	34.46	32.16	29.37	32.65	31.35	29.83	28.06	37.40	36.72	35.89	34.91
1000	39.22	37.13	34.62	31.59	35.37	33.89	32.19	30.22	40.38	39.67	38.82	37.82
1100	41.94	39.68	36.97	33.72	37.98	36.33	34.44	32.29	43.22	42.49	41.61	40.59
1200	44.55	42.13	39.24	35.78	40.48	38.67	36.62	34.29	45.95	45.18	44.29	43.25

[a] The viscosity values should be scaled using Equations (12), (14), and (15) to obtain the recommended values. The relative combined expanded (k = 2) uncertainty of the scaled values is 1.0% for 300 $\leqslant$ T/K $\leqslant$ 700, 1.5% for 200 $\leqslant$ T/K < 300 and 700 < T/K $\leqslant$ 1200, and 2.5% for 150 $\leqslant$ T/K < 200.

Table 5: Calculated values for the thermal conductivity, λ, of (CH_4 + CO_2), (CH_4 + H_2S), and (H_2S + CO_2) mixtures in the dilute gas limit as a function of mole fraction and temperature.[a]

T/K	λ/(mW·m^{-1}·K^{-1})											
	CH_4 (1) + CO_2 (2)				CH_4 (1) + H_2S (2)				H_2S (1) + CO_2 (2)			
	x_1 = 0.2	x_1 = 0.4	x_1 = 0.6	x_1 = 0.8	x_1 = 0.2	x_1 = 0.4	x_1 = 0.6	x_1 = 0.8	x_1 = 0.2	x_1 = 0.4	x_1 = 0.6	x_1 = 0.8
150	8.217	9.916	11.77	13.81	8.357	10.10	11.97	13.95	6.813	6.880	6.880	6.828
175	9.809	11.80	13.96	16.32	9.783	11.85	14.07	16.43	8.141	8.187	8.143	8.029
200	11.54	13.79	16.24	18.89	11.25	13.65	16.21	18.93	9.605	9.613	9.504	9.304
225	13.39	15.91	18.62	21.55	12.78	15.50	18.41	21.50	11.19	11.15	10.96	10.65
250	15.35	18.13	21.12	24.33	14.38	17.43	20.70	24.16	12.88	12.78	12.50	12.07
273.15	17.27	20.30	23.55	27.03	15.92	19.31	22.93	26.75	14.52	14.36	13.98	13.45
298.15	19.42	22.75	26.30	30.09	17.67	21.43	25.45	29.70	16.36	16.12	15.65	14.99
325	21.82	25.49	29.41	33.58	19.64	23.84	28.32	33.06	18.39	18.08	17.50	16.71
350	24.12	28.15	32.44	37.00	21.55	26.19	31.14	36.37	20.32	19.94	19.27	18.36
375	26.48	30.89	35.59	40.58	23.53	28.64	34.08	39.85	22.28	21.84	21.08	20.05
400	28.89	33.71	38.85	44.31	25.59	31.18	37.15	43.48	24.26	23.75	22.91	21.77
425	31.33	36.60	42.21	48.17	27.70	33.81	40.33	47.25	26.25	25.69	24.76	23.52
450	33.80	39.54	45.65	52.15	29.87	36.51	43.61	51.14	28.25	27.63	26.64	25.30
475	36.29	42.52	49.17	56.23	32.08	39.29	46.99	55.15	30.25	29.59	28.53	27.10
500	38.81	45.55	52.75	60.40	34.34	42.12	50.44	59.26	32.26	31.55	30.42	28.93
550	43.86	51.70	60.06	68.98	38.98	47.96	57.55	67.74	36.26	35.48	34.25	32.62
600	48.94	57.93	67.54	77.81	43.76	53.97	64.89	76.50	40.23	39.40	38.10	36.36
650	54.01	64.22	75.14	86.84	48.64	60.13	72.41	85.50	44.17	43.31	41.96	40.15
700	59.07	70.53	82.83	96.00	53.62	66.41	80.09	94.67	48.06	47.19	45.82	43.98
750	64.09	76.86	90.57	105.3	58.67	72.78	87.88	104.0	51.90	51.05	49.68	47.82
800	69.07	83.17	98.33	114.6	63.77	79.22	95.75	113.4	55.68	54.86	53.51	51.67
900	78.87	95.73	113.9	133.4	74.06	92.22	111.7	132.4	63.06	62.35	61.11	59.36
1000	88.42	108.1	129.3	152.2	84.37	105.2	127.6	151.5	70.18	69.64	68.56	66.97
1100	97.71	120.2	144.5	170.9	94.60	118.2	143.5	170.5	77.04	76.70	75.84	74.45
1200	106.7	132.1	159.5	189.2	104.7	131.0	159.1	189.2	83.65	83.54	82.92	81.78

[a] The thermal conductivity values should be scaled using Equations (13) and (16) to obtain the recommended values. The relative combined expanded (k = 2) uncertainty of the scaled values is 2.0% for 300 $\leqslant T$/K $\leqslant$ 700, 2.5% for 200 $\leqslant T$/K < 300 and 700 < T/K $\leqslant$ 1200, and 3.5% for 150 $\leqslant T$/K < 200.

Table 6: Calculated values for the product of molar density and binary diffusion coefficient, $\rho_m D$, of the (CH_4 + CO_2), (CH_4 + H_2S), and (H_2S + CO_2) systems in the dilute gas limit as a function of mole fraction and temperature.[a]

T/K	$10^4 \times \rho_m D$/(mol·m^{-1}·s^{-1})								
	CH_4 (1) + CO_2 (2)			CH_4 (1) + H_2S (2)			H_2S (1) + CO_2 (2)		
	$x_1 \to 0$	$x_1 = 0.5$	$x_1 \to 1$	$x_1 \to 0$	$x_1 = 0.5$	$x_1 \to 1$	$x_1 \to 0$	$x_1 = 0.5$	$x_1 \to 1$
150	3.689	3.687	3.686	3.701	3.701	3.701	2.291	2.285	2.281
175	4.354	4.353	4.352	4.360	4.361	4.361	2.734	2.728	2.724
200	5.008	5.008	5.008	5.008	5.009	5.009	3.191	3.184	3.181
225	5.646	5.647	5.647	5.641	5.642	5.643	3.652	3.647	3.644
250	6.266	6.267	6.267	6.257	6.258	6.259	4.114	4.109	4.107
273.15	6.822	6.823	6.823	6.813	6.813	6.814	4.538	4.534	4.533
298.15	7.403	7.404	7.403	7.396	7.396	7.396	4.989	4.987	4.986
325	8.006	8.006	8.004	8.005	8.004	8.003	5.464	5.463	5.463
350	8.549	8.548	8.544	8.555	8.554	8.552	5.896	5.896	5.897
375	9.075	9.073	9.067	9.091	9.088	9.085	6.317	6.318	6.320
400	9.586	9.582	9.573	9.613	9.609	9.604	6.728	6.730	6.732
425	10.08	10.08	10.06	10.12	10.12	10.11	7.128	7.131	7.133
450	10.56	10.56	10.54	10.62	10.61	10.60	7.518	7.521	7.524
475	11.03	11.02	11.01	11.11	11.10	11.09	7.898	7.902	7.905
500	11.49	11.48	11.46	11.58	11.57	11.56	8.269	8.272	8.276
550	12.38	12.36	12.33	12.51	12.49	12.47	8.983	8.987	8.991
600	13.22	13.20	13.16	13.39	13.38	13.35	9.666	9.670	9.673
650	14.04	14.01	13.97	14.25	14.23	14.20	10.32	10.32	10.33
700	14.82	14.79	14.74	15.09	15.06	15.02	10.95	10.95	10.95
750	15.59	15.55	15.49	15.89	15.86	15.82	11.55	11.56	11.56
800	16.32	16.28	16.22	16.68	16.64	16.59	12.14	12.14	12.15
900	17.74	17.69	17.61	18.20	18.15	18.09	13.26	13.27	13.27
1000	19.10	19.04	18.94	19.65	19.60	19.52	14.33	14.33	14.33
1100	20.40	20.33	20.22	21.05	20.99	20.90	15.34	15.35	15.34
1200	21.65	21.57	21.46	22.40	22.33	22.24	16.32	16.32	16.32

[a] The relative combined expanded ($k = 2$) uncertainty is 2.0% for $300 \leqslant T/\mathrm{K} \leqslant 700$, 2.5% for $200 \leqslant T/\mathrm{K} < 300$ and $700 < T/\mathrm{K} \leqslant 1200$, and 3.5% for $150 \leqslant T/\mathrm{K} < 200$.